ORNL/TM-2022/2458

Oak Ridge National Laboratory Detector Characterization for Accurate Monte Carlo Simulation and Neutron Energy-spectrum Unfolding

J. Nattress
P. Rose
P. Hausladen

June 2022

OAK RIDGE NATIONAL LABORATORY
MANAGED BY UT-BATTELLE FOR THE US DEPARTMENT OF ENERGY

ORNL/TM-2022/2458

Physics Division

Detector Characterization for Accurate Monte Carlo Simulation and Neutron Energy-spectrum Unfolding

J. Nattress, P. Rose, and P. Hausladen

Date Published: June 2022

Prepared by
OAK RIDGE NATIONAL LABORATORY
Oak Ridge, TN 37831-6283
managed by
UT-Battelle, LLC
for the
US DEPARTMENT OF ENERGY
under contract DE-AC05-00OR22725

CONTENTS

LIST OF FIGURES

ABSTRACT

This report details the characterization of a deuterated scintillation detector for use in neutron spectroscopy via the spectrum unfolding technique. The active volume of the detector consists of a 3-in. diameter by 3 in. depth right circular cylinder that contains 337 cm^3 of liquid scintillator EJ-315, deuterated benzene with a D:H ratio of 141:1. A deuterated scintillator is desirable for unfolding fast neutron energy spectra because the backscattering of neutrons from deuterium produces peaks in the pulse height response corresponding to the incident neutron energy. Spectrum unfolding requires the detector's response to be accurately known for any input neutron energy. The characterization in this report supports using a simulated response matrix calibrated by the measured light output and convolved with the measured resolution to produce a response matrix without bringing the detector to a neutron beam facility for characterization. In particular, characterization measurements were performed that included calibration of the detector's light output to recoil electrons from gamma sources, calibration of the detector's resolution to recoil electrons, and calibration of the detector's light output to recoil protons from a time-tagged neutron source and a monoenergetic 14.1 MeV neutron source.

1. Introduction

The ability to accurately measure neutron energy (neutron spectroscopy) could prove useful for a variety of security applications [18, 4, 14]. As a result, the authors have been investigating the use of neutron spectroscopy via spectrum unfolding for various applications, such as to improve material identification [15] and to reduce uncertainty with neutron multiplicity counting. Previous work has performed spectrum unfolding based on a measured response matrix [9]. Although a measured response is preferred, it is cumbersome (in cost, effort, and scheduling) to directly measure the response of the detector for the required number of discrete neutron energies each with the desired counting statistics. The present work considers use of simulated response matrices that are calibrated by more attainable experimental results. Unfolding via the resultant response matrix has proven to achieve similar performance for fission-spectrum neutrons while alleviating some of the burden of calibration. The present work focuses on the characterization of an organic liquid scintillator detector to support accurate Monte Carlo modeling. In particular, a 3-in. diameter by 3 in. depth right-cylinder of EJ-315 deuterated benzene liquid scintillator was characterized and the results presented herein. Note that the methods presented are more broadly applicable to aid the accurate simulation of scintillation detector response.

Organic liquid scintillators are used extensively for security and basic science applications. The more widely-used, conventional, hydrogen-based detectors rely on *n-p* scattering for detection of neutrons, which is isotropic in the center-of-mass frame. The isotropic characteristic of this reaction results in a relatively "flat" response to monoenergetic neutrons; that is, pulse heights up to the incident neutron energy are approximately equally likely. Deuterated liquid scintillators and crystals have found application to determining neutron energy spectra via unfolding techniques [2]. These detectors preferentially rely on non-isotropic *n-d* back-scattering; this asymmetry results in distinct peaks in the observed light-output spectrum for discrete neutron energies. The result of the "more peaked" spectrum improves the condition number of the response matrix, leading to improved unfolding performance for complicated spectra [7, 13, 8]. This "more peaked" light output may also improve the performance of *spectrum stripping*, an alternative method for performing neutron spectroscopy under certain input energy spectrum conditions [11].

2. Materials and Methods

The accurate simulation of a detector's response to neutrons and photons requires two main parameters to be measured–detector resolution and the particle specific, energy dependent light-output response. The measurements discussed in this report were performed with a 3-in right cylinder EJ-315 detector housed in an aluminum light-tight container with a borosilicate glass window. An ETEL 9821KB07 photomultiplier tube (PMT) was optically coupled to the window by an EJ-560 silicone rubber optical interface. A mu-metal shield surrounds the PMT. The detector assembly is commercially available from Eljen Technologies and can be purchased either as a full assembly or as individual components.

Signals produced from the detector were recorded by a CAEN DT5730 8-channel, 14-bit, 500-MHz waveform digitizer. The CAEN Multi-PArameter Spectroscopy Software (CoMPASS) was used to record full waveform data; the recorded waveforms were 498 points or 992 ns in length. Data were post-processed to identify events corresponding to neutrons and photons via the charge integration method. An example of particle identification via this method is shown in 1. The PSD metric on the vertical axis in is defined as

$$PSD = Q_{short}/Q_{long}, \tag{1}$$

where Q_{long} is the total charge collected in a 200 ns window starting 40 ns before the peak and Q_{short} is the charge collected in a time window starting 22 ns from the peak to the same endpoint as Q_{long}. While a longer integration window is typically desirable, no PSD optimization was performed in this work, as these baseline values were sufficient for the analysis. Standard pulse processing algorithms were applied to remove pile-up and pulses that exceeded the dynamic range of the digitizer. Conservative graphical cuts were applied to the appropriate regions in Fig. 1 to identity each event as a neutron or a photon.

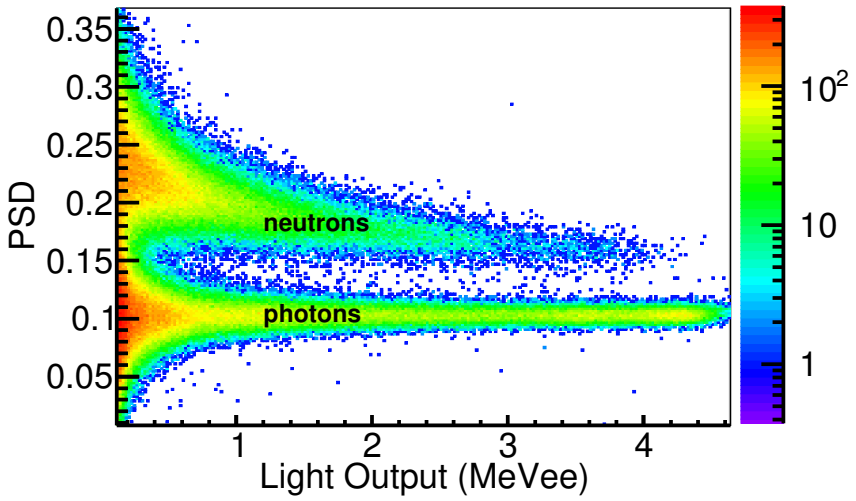

Figure 1. Response of a 3-in EJ-315 detector for an Am-Be radioisotope source.

For performing calibration of pulse heights in "electron equivalent" energies and for quantifying detector resolution, data were taken individually with ^{22}Na, ^{137}Cs, and Am-Be radioisotope sources. Conversion to electron equivalent energy was calculated by locating the point on the horizontal axis corresponding to a

number of counts equal to 80% of maximum number of counts located at the high-edge (C_m) of the recorded ^{137}Cs light-output spectrum. This point was equated to the Compton edge energy of 477 keV by convolving the calculated energy spectrum with the measured resolution. The selection process for the point is graphically shown in Fig. 2, which shows a simulated deposited-energy spectrum that has been convolved with a measured resolution function. Overlaid on the figure is the deposited energy in the detector. All results were converted to electron equivalent energy using this technique with checks for PMT drift performed on each day of an individual measurement.

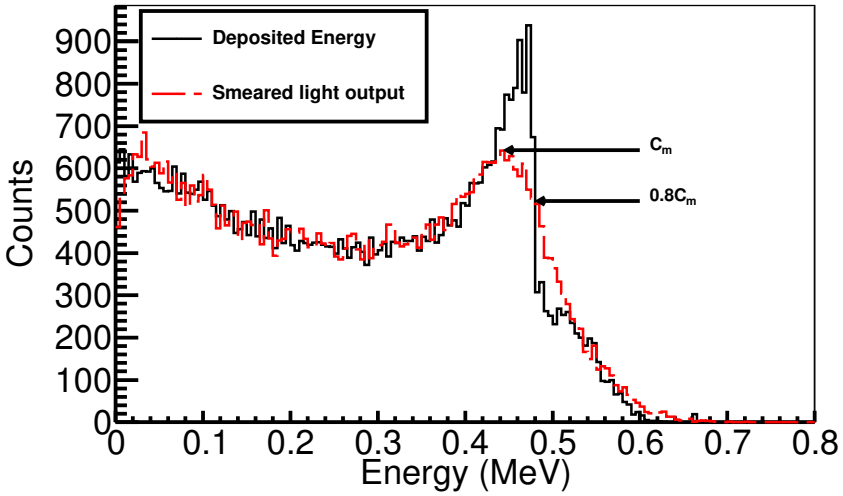

Figure 2. Simulated energy deposited in a 3-in EJ-315 detector (red) and the convolved detector response (black) when exposed to a ^{137}Cs radioisotope source.

The resolution for a discrete gamma-ray energy was calculated with the method outlined by V. Bildstein [3]. This method defined the resolution (in percent) as

$$R = 100\left|\frac{C_{12.5} - C_{87.5}}{C_{50}}\right|, \tag{2}$$

where where C_x is the channel at which the number of counts is x percent of the number of counts at the observed Compton maximum peak, just below the position of the Compton edge. The aforementioned gamma-ray sources provide 4 points to determine resolution using the characteristic energies of the Compton edges: 0.511 MeV (^{22}Na), 0.622 MeV ^{137}Cs, 1.274 MeV (^{22}Na), and 4.43 MeV (Am-Be).

The detector's neutron energy-dependent light-output response was measured via time-of-flight (TOF). A ^{252}Cf fission chamber was used for this measurement. The fission chamber uses the fission signal to provide a start time to measure the TOF of the emitted neutrons. A flight path of 1 m was used. The energy of neutron events, E_n, (determined by their TOF) was calculated from

$$E_n = \frac{mc^2}{\sqrt{1 - v^2/c^2}}, \tag{3}$$

where m is the mass of a neutron, v is the neutron's velocity ($v = L/TOF$, and L is the distance from the origin of the neutron to the detector), and c is the speed of light.

3. Results

3.1 Detector Resolution

The detector resolution, $\Delta L/L$, is described with a Gaussian broadening model, which was applied event-by-event:

$$\frac{\Delta L}{L} = \sqrt{\alpha^2 + \frac{\beta^2}{L} + \left(\frac{\gamma}{L}\right)^2}. \tag{4}$$

Equation (2) [5, 16, 17] is a conventional parameterization, where α is attributed to position-dependent light transmission between the scintillator and the photocathode, β accounts for the statistical nature of the photon production and attenuation of light in the scintillator (including the quantum efficiency and electron amplification of the PMT), and γ is due to the electronic noise of the PMT and waveform digitizer [6]. The measured resolutions and light outputs corresponding to the gamma-ray sources mentioned in the previous section were fit to equation 4. The results of the fit are shown in Figure 3. A Geant4 [1] Monte Carlo simulation of a ^{137}Cs point source incident onto a 3-in EJ-315 detector was performed to validate the resolution parameters. The results of the validation are shown in Figure 4, indicating good agreement from 0.2 MeVee and above. Dissimilarities seen at low light-output values can be attributed to scattering objects such as the floor, table, and electronics that were present in the measurement and absent in the simultions.

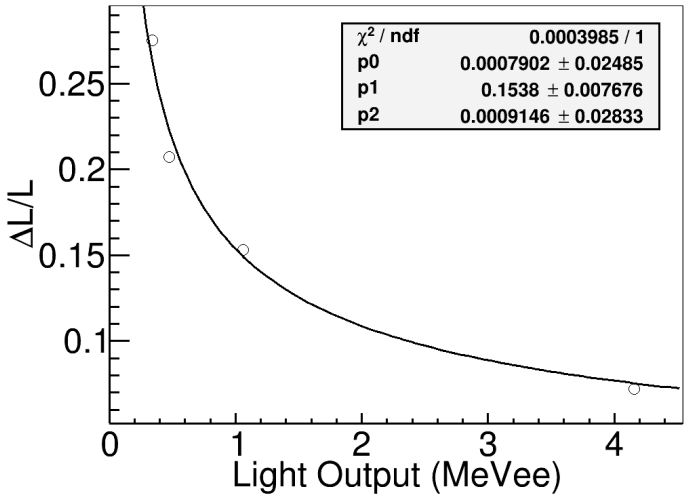

Figure 3. Resolution fundtion for the 3-in EJ-315 detector.

3.2 Light Output Characterization

The deuteron light-output response of the detector was measured using a ^{252}Cf fission chamber and a DT-neutron generator. The results of the ^{252}Cf experiment are shown in Figure 5. The expected nonlinear correlation between the observed light output and neutron energy is evident in the figure. The bulk of events occurs at or below 2 MeV due to the spectral shape of the ^{252}Cf fission and the inverse proportionality between detector efficiency as neutron energy.

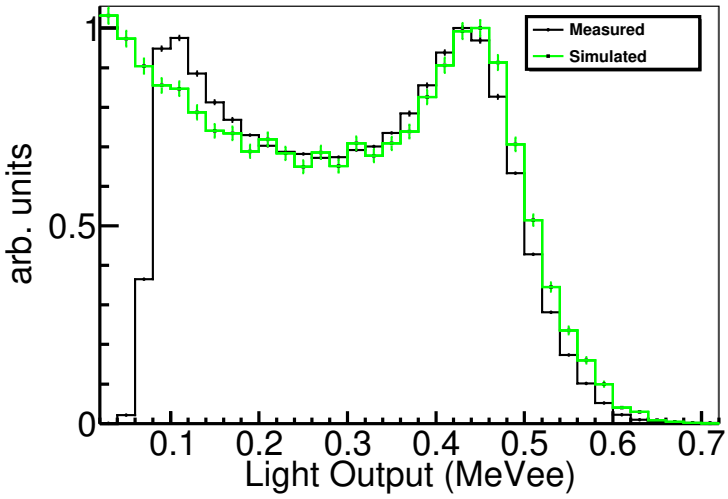

Figure 4. Simulated analytically convolved (green) and measured (black) light-output distribution observed with a 3-in right-cylinder EJ-315 detector when irradiated by a ^{137}Cs source.

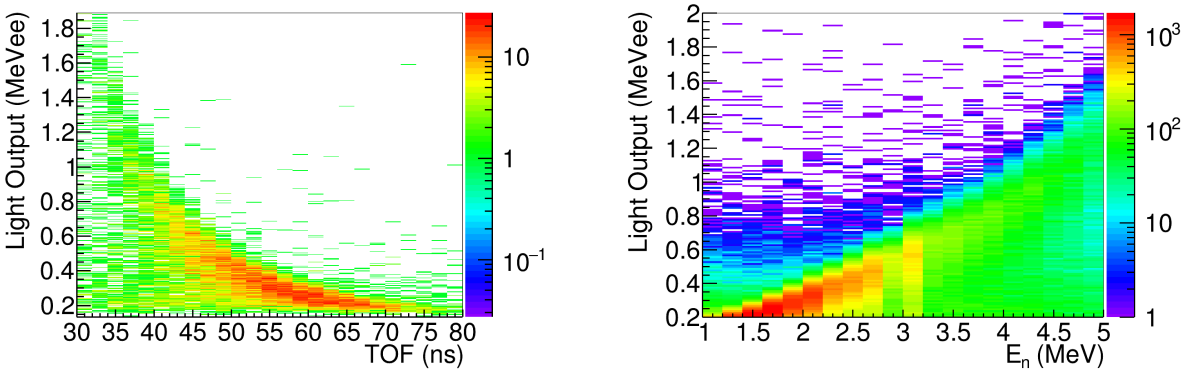

Figure 5. Light output as a function of time-of-flight (TOF) (left) and light output as a function of the calculated neutron energy (right) for a EJ-315 detector exposed to a ^{252}Cf radioisotope source.

Slices of light-output spectra were extracted from the TOF data from 2 to 5 MeV with an energy bin width of 0.12 MeV. The center of the bin was selected as the energy point for a given distribution. An example of an extracted slice is shown in Figure 6 for 3.83 MeV neutrons. A procedure analogous to that used to determine the energy of the Compton edge was employed to determine the pulse height corresponding to full-energy deposition of neutrons, but for neutron-deuteron scattering, 50% of the count maximum at the high-energy region corresponds to the neutron's full energy deposition on a deuteron. Additionally, the full-energy deposition point from a 14.1-MeV neutron originating from the D-T reaction was identified. From the TOF slices and the DT neutron light output distribution, the light output as a function of recoiling deuteron energy was determined. The results of this determination is shown in Figure 7 along with several other EJ-315 characterizations taken from the literature. A 5% uncertainty is assigned to all data sets.

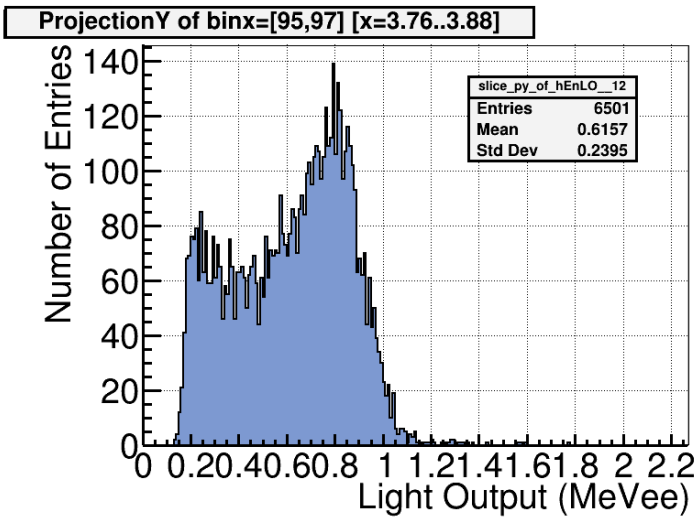

Figure 6. Light-output slice extracted centered at 3.82 MeV and accepting energies within the range of 3.76 to 3.88.

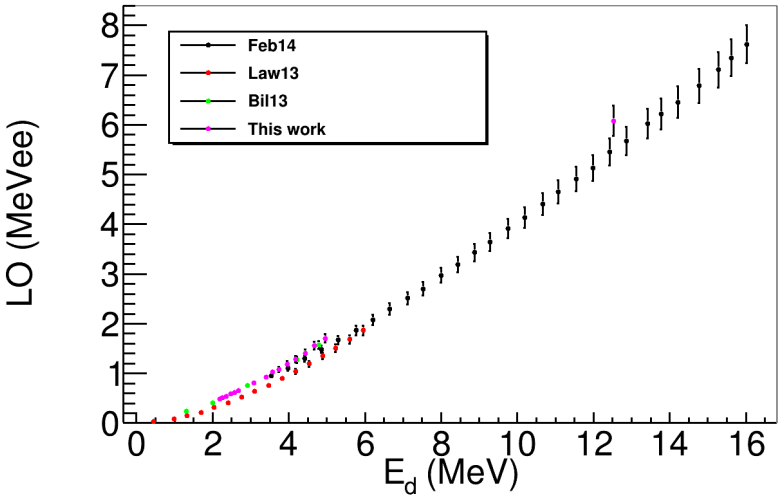

Figure 7. Comparison of light-response data for EJ-315 scintillators including this work [10, 12, 3].

The functional form

$$L(E_d) = p0 \cdot E_d + p1(1 - e^{p2 \cdot E_d}) \tag{5}$$

was fit to the light-output response function in Figure 8, where the fitting parameters are listed on the figure.

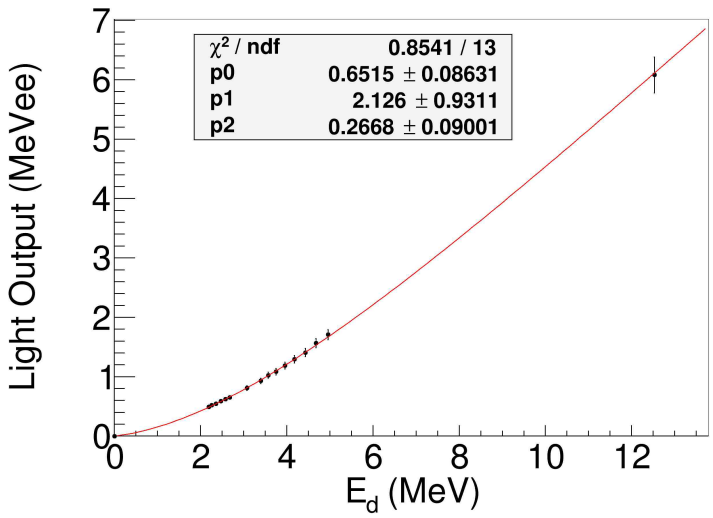

Figure 8. Light-output respnse curve from TOF and DT neutron data, where the points corrrespond to 50% of the maximum recoil peak height.

3.3 Response Matrix

A response matrix was simulated using Geant4.10.05.p01. For this simulation, a neutron beam was directed at the detector's face so that every source neutron was within the solid angle of the detector. The detector response to monoenergetic neutrons was simulated for 380 energies from 1.1 to 20 MeV in 50 keV increments. The energy deposited for individual deuteron tracks was tallied on an event-by-event basis. Using the resolution and light output parameterizations inferred from measurements, each track was converted to light output and then convolved with the measured resolution function. This process was executed at run time to take advantage of Geant4's inherent multi-threading capability to speed up the total processing time. The final response matrix is shown in Figure 9.

3.4 Unfolding

The neutron light response to 14.1-MeV neutrons from the DT measurement was unfolded using the maximum-likelihood expectation-maximization method (MLEM) to evaluate the accuracy of the simulated response matrix. MLEM is a Bayesian method used to infer underlying probability distribution parameters of a particular data set. The MLEM equations are solved on a case-by-case basis for a given likelihood function based on its intrinsic probability distributions. In the case of neutron energy-spectrum unfolding, more specifically organic scintillators, the MLEM algorithm is represented in an iterative form as follows:

$$x_j^{(k+1)} = \frac{x_j^{(k)}}{\sum_i R_{ij}} \sum_i R_{ij} \frac{s_i}{\sum_l R_{il} x_l^{(k)}}, \tag{6}$$

where s_i is the measured light-output, R_{ij} is the detector response matrix, x_j is the estimated unfolded neutron energy spectrum for iteration k [8].

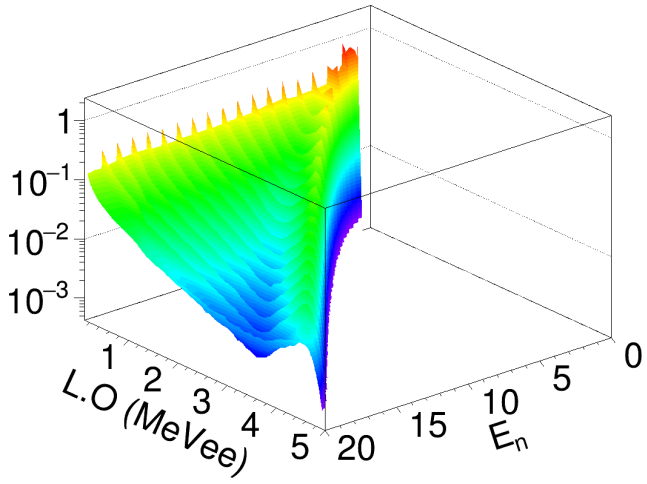

Figure 9. Response matrix for the deuterated EJ-315 generated using Geant4.

Figure 10 shows the unfolded neutron energy results from the DT measurement. The energy distribution is in good agreement with the expected energy from the DT fusion reaction of 14.1 MeV. There is also good agreement between the projected light-output distribution and the measured. A quantitative comparison between the two light-output distributions is shown in Figure 11, where the difference between the measured light-output spectrum and the projected light-output (σ) divided by the square root of the measured counts is displayed.

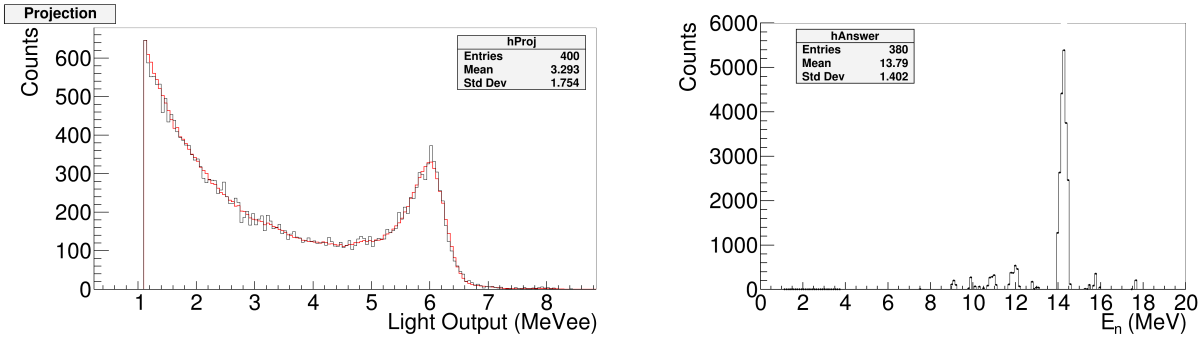

Figure 10. The projected light-output spectrum (red) compared to the measured spectrum (black) (left). Unfolded neutron energy spectrum (right).

4. Conclusions

A detector whose active volume comprised a 3-in. diameter by 3 in. depth right circular cylinder of liquid scintillator EJ-315 was characterized using several gamma-ray and neutron radioisotope sources. The resolution was measured at several energies between 0 and 4 MeV. A ^{252}Cf fission chamber was used to determine the light-output response of the detector to neutron energies between approximately 2 and 5

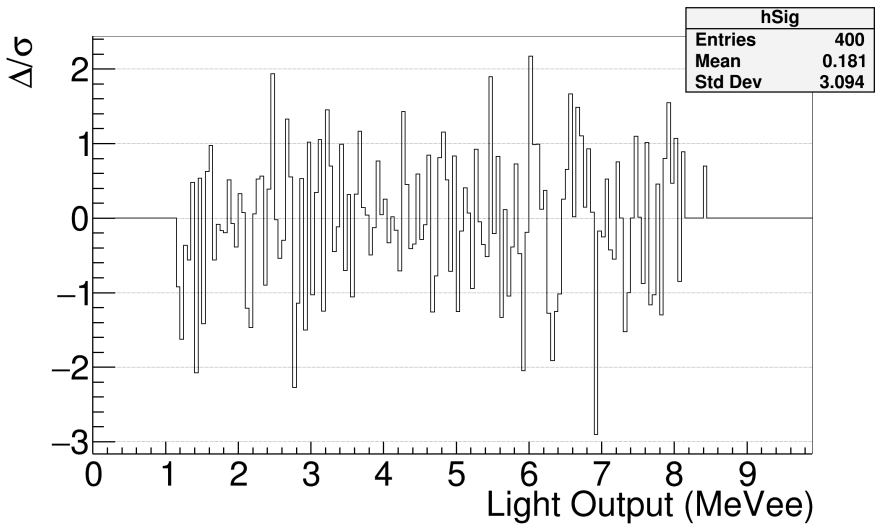

Figure 11. The difference between the measured light-output spectrum and the projected light-output divided by the square root of the measured counts.

MeV. The response to 14.1 MeV neutrons was also determined. The light-output response and resolution were parameterized using well-known functional forms and combined with Geant4 radiation transport simulations to produce a simulated response matrix. Neutron energy-spectrum unfolding was demonstrated for a monoenergetic neutron source via the MLEM algorithm. The response matrix development process will be used to characterize other organic scintillators that will be used for other unfolding applications.

References

[1] S. Agostinelli, J. Allison, K. a. Amako, J. Apostolakis, H. Araujo, P. Arce, M. Asai, D. Axen, S. Banerjee, G. Barrand, et al. Geant4âĂŤa simulation toolkit. *Nuclear instruments and methods in physics research section A: Accelerators, Spectrometers, Detectors and Associated Equipment*, 506(3):250–303, 2003.

[2] F. Becchetti, R. Raymond, R. Torres-Isea, A. Di Fulvio, S. Clarke, S. Pozzi, and M. Febbraro. Deuterated-xylene (xylene-d10; ej301d): A new, improved deuterated liquid scintillator for neutron energy measurements without time-of-flight. *Nuclear Instruments and Methods in Physics Research Section A: Accelerators, Spectrometers, Detectors and Associated Equipment*, 820:112–120, 2016.

[3] V. Bildstein, P. Garrett, J. Wong, D. Bandyopadhyay, J. Bangay, L. Bianco, B. Hadinia, K. Leach, C. Sumithrarachchi, S. Ashley, et al. Comparison of deuterated and normal liquid scintillators for fast-neutron detection. *Nuclear Instruments and Methods in Physics Research Section A: Accelerators, Spectrometers, Detectors and Associated Equipment*, 729:188–197, 2013.

[4] D. L. Chichester, J. T. Johnson, and E. H. Seabury. High-resolution fast-neutron spectrometry for arms control and treaty verification. Technical report, Idaho National Laboratory (INL), 2012.

[5] G. Dietze. Energy calibration of NE-213 scintillation counters by δ-rays. *IEEE Trans. Nucl. Sci.*, 26(1):398–402, 1979.

[6] G. Dietze and H. Klein. Gamma-calibration of NE 213 scintillation counters. *Nucl. Instrum. Methods Phys. Res.*, 193(3):549–556, 1982.

[7] M. Febbraro, F. Becchetti, R. Torres-Isea, J. Riggins, C. Lawrence, J. Kolata, and A. Howard. (d, n) proton-transfer reactions on be 9, b 11, c 13, n 14, 15, and f 19 and spectroscopic factors at e d= 16 mev. *Physical Review C*, 96(2):024613, 2017.

[8] M. Febbraro, B. Becker, R. deBoer, K. Brandenburg, C. Brune, K. Chipps, T. Danley, A. Di Fulvio, Y. Jones-Alberty, K. Macon, et al. Performance of neutron spectrum unfolding using deuterated liquid scintillator. *Nuclear Instruments and Methods in Physics Research Section A: Accelerators, Spectrometers, Detectors and Associated Equipment*, 989:164824, 2021.

[9] M. Febbraro, R. Toomey, S. Pain, K. Chipps, B. Becker, R. Newby, Z. Meisel, T. Massey, C. Brune, Q. Liu, et al. The ornl deuterated spectroscopic arrayâĂŤodesa. *Nuclear Instruments and Methods in Physics Research Section A: Accelerators, Spectrometers, Detectors and Associated Equipment*, 946:162668, 2019.

[10] M. T. Febbraro. *A Deuterated Neutron Detector Array for the Study of Nuclear Reactions with Stable and Rare Isotope Beams.* PhD thesis, 2014.

[11] G. F. Knoll. *Radiation detection and measurement*. 2010.

[12] C. C. Lawrence. *Neutron Spectrum Unfolding with Organic Scintillators for Arms-control Verification.* PhD thesis, 2014.

[13] C. C. Lawrence, A. Enqvist, M. Flaska, S. A. Pozzi, A. Howard, J. Kolata, and F. Becchetti. Response characterization for an ej315 deuterated organic-liquid scintillation detector for neutron spectroscopy. *Nuclear Instruments and Methods in Physics Research Section A: Accelerators, Spectrometers, Detectors and Associated Equipment*, 727:21–28, 2013.

[14] J. Nattress, T. Nolan, S. McGuinness, P. Rose, A. Erickson, G. Peaslee, and I. Jovanovic. High-contrast material identification by energetic multiparticle spectroscopic transmission radiography. *Physical Review Applied*, 11(4):044085, 2019.

[15] J. Nattress and P. Rose Jr. Material identification via dual particle transmission using a radioisotope source. Technical report, Oak Ridge National Lab.(ORNL), Oak Ridge, TN (United States), 2021.

[16] H. Schölermann and H. Klein. Optimizing the energy resolution of scintillation counters at high energies. *Nucl. Instrum. Methods*, 169(1):25–31, 1980.

[17] P. Sparrman, J. Lindskog, and A. Marelius. An electron scintillation detector with good energy resolution. *Nucl. Instrum. Methods*, 41(2):299–304, 1966.

[18] T. Zak, S. D. Clarke, M. M. Bourne, S. A. Pozzi, Y. Xu, T. J. Downar, and P. Peerani. Neutron spectroscopy of plutonium oxide using matrix unfolding approach. *Nuclear Instruments and Methods in Physics Research Section A: Accelerators, Spectrometers, Detectors and Associated Equipment*, 622(1):191–195, 2010.